

# Self-organized thermosets involving epoxy and poly( $\epsilon$ -caprolactone)-*block*-poly(ethylene-*co*-ethylethylene)-*block*-poly( $\epsilon$ -caprolactone) amphiphilic triblock copolymer

Di Hu, Chongyin Zhang, Rentong Yu, Lei Wang, Sixun Zheng\*

Department of Polymer Science and Engineering and State Key Laboratory of Metal Matrix Composites, Shanghai Jiao Tong University, Shanghai 200240, PR China

## ARTICLE INFO

### Article history:

Received 27 July 2010

Received in revised form

7 October 2010

Accepted 10 October 2010

Available online 16 October 2010

### Keywords:

Epoxy

Triblock copolymer

Self-assembly

## ABSTRACT

In this work, we investigated the self-assembly behavior of poly( $\epsilon$ -caprolactone)-*block*-poly(ethylene-*co*-ethylethylene)-*block*-poly( $\epsilon$ -caprolactone) (PCL-*b*-PEEE-*b*-PCL) triblock copolymer in epoxy thermosets. The PCL-*b*-PEEE-*b*-PCL triblock copolymer was synthesized *via* the ring-opening polymerization of  $\epsilon$ -caprolactone with a hydroxyl-terminated poly(ethylene-*co*-ethylethylene) as the macromolecular initiator. The hydroxyl-terminated poly(ethylene-*co*-ethylethylene) was prepared with the hydrogenation reaction of a hydroxyl-terminated polybutadiene. The triblock copolymer was incorporated into the precursors of epoxy to obtain the nanostructured thermosets. It was found that the self-organized nanophases were formed in the mixture before curing reaction and the nanostructures can be further fixed *via* curing reaction. The self-assembly behavior of the triblock copolymer in epoxy thermosets was investigated by means of atomic force microscopy (AFM), small-angle X-ray scattering (SAXS) and dynamic mechanical thermal analysis (DMTA). Differential scanning calorimetry (DSC) shows that the formation of the self-organized nanophase in the thermosets caused that a part of poly( $\epsilon$ -caprolactone) subchains were demixed from epoxy matrix with the occurrence of curing reaction; the fractions of demixed PCL blocks were estimated according to the  $T_g$ -composition relation of the model binary blends of epoxy and PCL.

© 2010 Elsevier Ltd. All rights reserved.

## 1. Introduction

Incorporating block copolymers into thermosets has been proved to be an efficient approach to obtain ordered or disordered nanostructures into the materials [1,2]. Hillmyer et al. [3,4] first reported a self-assembly approach by the use of amphiphilic block copolymers. In this protocol, the precursors of thermosets act as selective solvents of the block copolymers and some self-organized morphologies such as lamellar, bicontinuous, cylindrical, and spherical nanophases are formed depending on the composition of the mixtures; these nanophases can be further fixed by adding hardeners and subsequent curing reaction [5–25]. The role of curing reaction is to lock in the morphology that is already present. Therefore, the self-assembly approach is a typical template-based technique. More recently, it was demonstrated that ordered and/or disordered nanophases in thermosets can be alternatively formed *via* the mechanism of reaction-induced microphase separation (RIMPS) [26,27]. In this approach, it is not required that the amphiphilic block copolymers are self-organized into the nanophases before curing

reaction, *i.e.*, all the subchains of block copolymers may be miscible with precursors of thermosets. Upon curing, a part of subchains of block copolymers are microphase-separated out from the thermosetting matrix whereas other subchains of the block copolymers remain miscible with the matrix of thermosets [18,28–36]. The formation mechanism of nanostructures in thermosets by the use of block copolymer is quite dependent on miscibility of block copolymer subchains with precursors of thermosets after and before curing reaction. The miscibility can be described in terms of several pairs of intermolecular Flory–Huggins interaction parameters in the mixture of precursors of thermosets and subchains of block copolymer [37], which are governed by the chemical structure of the related polymers. Therefore, these interaction parameters can be changed *via* the structural modification of existing copolymers. Under this circumstance, the formation mechanism of nanostructures in thermosets might be thus modulated by modifying the structure of an existing block copolymer.

In a previous work, we have demonstrated that the formation of nanostructures in epoxy thermosets containing poly( $\epsilon$ -caprolactone)-*block*-polybutadiene-*block*-poly( $\epsilon$ -caprolactone) (PCL-*b*-PB-*b*-PCL) triblock copolymer followed the mechanism of reaction-induced microphase separation [26]. It was found that all the subchains (*viz.* PB and PCL) of the triblock copolymer were miscible with

\* Corresponding author. Tel.: +86 21 54743278; fax: +86 21 54741297.  
E-mail address: [szheng@sjtu.edu.cn](mailto:szheng@sjtu.edu.cn) (S. Zheng).

the precursors (*viz.* DGEBA and MOCA) at the curing temperature, *i.e.*, no pre-formed self-assembly structures were formed at the beginning of curing reaction. With the curing reaction proceeding, the PB subchains were microphase-separated out from epoxy matrix whereas the PCL subchains remained miscible with epoxy matrix. It is of interest to note that the midblock (*viz.* PB) of the PCL-*b*-PB-*b*-CL triblock copolymer can be readily modified *via* the reaction of hydrogenation, *i.e.*, the unsaturated polyolefin (*viz.* PB) can be reduced into a saturated carbon-hydrogen polymer, *i.e.*, ethylene-*co*-ethylethylene copolymer (PEEE). The transformation from an unsaturated to a saturated polyolefin could give rise to a significant change in solubility parameters since most of saturated polyolefinic polymers (*e.g.*, polyethylene, polyethylethylene) are immiscible with epoxy, which is in marked contrast to unsaturated polyolefinic polymers (*e.g.*, PB). As a consequence, if any, the formation of the nanostructures in epoxy thermosets containing PCL-*b*-PEEE-*b*-PCL triblock copolymer will follow a self-assembly mechanism.

The purpose of this work is to demonstrate that the formation mechanism of the nanostructures in epoxy thermosets containing PCL-*b*-PEEE-*b*-PCL was shifted to self-assembly mechanism with the hydrogenation of polybutadiene blocks. Toward this end, the hydrogenation of the hydroxyl-terminated polybutadiene used in a previous work [26] was carried out to afford the hydroxyl-terminated poly(ethylene-*co*-ethylethylene), which was then used as the macromolecular initiator to obtain a PCL-*b*-PEEE-*b*-PCL triblock copolymer *via* ring-opening polymerization. Thereafter, the triblock copolymer was incorporated into epoxy resin to access the nanostructured thermosets. The morphology and formation mechanism of nanostructures was investigated by means of atomic force microscopy (AFM), small-angle X-ray scattering (SAXS) and dynamic mechanical thermal analysis (DMTA) and the self-assembly behavior of the triblock copolymer in epoxy resin was addressed. The demixing behavior of the miscible block (*viz.* PCL) was investigated in terms of the glass transition behavior of the nanostructured thermosets.

## 2. Experimental

### 2.1. Materials

Diglycidyl ether of bisphenol A (DGEBA) with epoxide equivalent weight of 185–210 was purchased from Shanghai Resin Co., China. 4,4'-Methylenebis(2-chloroaniline) (MOCA) and 3,5-di-*tert*-butyl-4-hydroxytoluene were of analytically pure grade, obtained from Shanghai Reagent Co., China. The monomer,  $\epsilon$ -caprolactone (CL), was purchased from Fluka Co., Germany and it was distilled over CaH<sub>2</sub> under decreased pressure before use. Stannous (II) octanoate [Sn(Oct)<sub>2</sub>] was of chemically pure grade, purchased from Shanghai Reagent Co., China. *p*-Toluenesulfonylhydrazide was purchased from Houli Trade Co., Ltd., Shanghai, China and used as received. The hydroxyl-terminated polybutadiene is the same as that used in a previous work [26] and it was kindly supplied by Qilong Chemical Co., Shandong, China and it was prepared *via* anionic polymerization. It has a quoted molecular weight of  $M_n = 3500$ . The <sup>1</sup>H-NMR spectroscopy showed that in its main-chain structure there are 20 mol % 1,2-addition and 80 mol % 1,4-addition structural units in which the content of *trans*-1,4 additional moieties is 60 mol %. All other reagents and solvents used in this work are obtained from commercial resources and were purified according to standard procedures prior to use.

### 2.2. Hydrogenation of hydroxyl-terminated polybutadiene

The hydrogenation of hydroxyl-terminated polybutadiene was carried out by following the literature method [38–41]. Typically, the hydroxyl-terminated polybutadiene (4.0 g, 1.1429 mmol) was

dissolved in anhydrous xylene (350 ml); *p*-toluenesulfonylhydrazide (66.2204 g, 0.3556 mol) and antioxidant 3,5-di-*tert*-butyl-4-hydroxytoluene (99.328 mg) were added. The mixture was refluxed at 120 °C under highly pure nitrogen for 15 h. The degree of hydrogenation was traced by means of Fourier transform infrared spectroscopy. After that, the solution was cooled to room temperature and half of the xylene was removed under reduced pressure. The concentrated solution was then precipitated into ice-cold methanol and the white solid [*i.e.*, hydroxyl-terminated poly(ethylene-*co*-ethylethylene)] was collected and dried at 40 °C in a vacuum oven for 36 h and 4.28 g product was obtained with the yield of 98%. It is noted that with the occurrence of hydrogenation, the product was no longer soluble in the solvents of polybutadiene such as tetrahydrofuran and chloroform but it can be dissolved in some non-polar solvents such as benzene, toluene and xylene. <sup>1</sup>H-NMR (ppm, C<sub>6</sub>D<sub>6</sub>): 0.91 [1H, CH<sub>3</sub>CH<sub>2</sub>C], 3.31 [19H, CH<sub>2</sub>OH]. The molecular weight of the hydroxyl-terminated poly(ethylene-*co*-ethylethylene) can be estimated to be  $M_n = 3680$  according to the ratio of integral intensity of methylene protons connected to the terminal hydroxyl groups at 3.31 ppm to other methylene protons in the <sup>1</sup>H-NMR spectrum of the product (See curve A in Fig. 2).

### 2.3. Synthesis of PCL-*b*-PEEE-*b*-PCL triblock copolymer

The PCL-*b*-PEEE-*b*-PCL triblock copolymer was synthesized *via* the ring-opening polymerization of  $\epsilon$ -caprolactone (CL) with the above hydroxyl-terminated poly(ethylene-*co*-ethylethylene) as the macromolecular initiator and stannous (II) octanoate [Sn(Oct)<sub>2</sub>] was used as the catalyst. Typically, the macromolecular initiator (1.5 g, 0.43 mmol), CL (3.0608 g, 2.86 mol) and anhydrous xylene (2 ml) were added to a pre-dried flask equipped with a magnetic stirrer. The flask was connected to a standard Schlenk line and the system was degassed *via* three pump-freeze-thaw cycles and then Sn(Oct)<sub>2</sub> [dissolved in anhydrous toluene, 1/1000 (wt) with respect to  $\epsilon$ -CL] was added using a syringe. With additional three pump-freeze-thaw cycle, the flask was immersed in a thermostated oil bath at 120 °C for 36 h to attain a complete polymerization. Cooled to room temperature, the crude product was dissolved in tetrahydrofuran (20 ml) and was precipitated in methanol (200 ml). The procedure of dissolving and precipitation was repeated thrice to purify the product and the product was dried in a vacuum oven at 30 °C for 36 h. The polymer (5.3 g) was obtained with the yield of 98.5%. <sup>1</sup>H-NMR (C<sub>6</sub>D<sub>6</sub>, ppm): 3.95 [4H, OCO(CH<sub>2</sub>)<sub>4</sub>CH<sub>2</sub>], 2.09 [4H, OCOCH<sub>2</sub>(CH<sub>2</sub>)<sub>4</sub>], 1.48 [8H, OCOCH<sub>2</sub>CH<sub>2</sub>CH<sub>2</sub>CH<sub>2</sub>CH<sub>2</sub>], 1.35 [4H, OCOCH<sub>2</sub>CH<sub>2</sub>CH<sub>2</sub>CH<sub>2</sub>CH<sub>2</sub>], 1.16 [4H, CH<sub>2</sub> connected to the methane in 1,4 structure,], 0.39 [3H, CH<sub>3</sub>CH<sub>2</sub>]. The length of PCL block in the triblock copolymer can be determined to be  $M_n$  (PCL) = 3610 in terms of the ratio of integral intensity of methylene protons connected to the terminal hydroxyl groups at 3.31 ppm to the methylene protons at 2.1 ppm of PCL in the <sup>1</sup>H-NMR spectrum of the product (See Fig. 3).

### 2.4. Synthesis of model Poly( $\epsilon$ -caprolactone)

The model PCL with the molecular weight identical with the length of PCL block in PCL-*b*-PEEE-*b*-PCL triblock copolymer was synthesized *via* the ring-opening polymerization (ROP) of  $\epsilon$ -CL with benzyl alcohol as the initiator. Typically, benzyl alcohol (0.21 g, 1.1 mmol) and  $\epsilon$ -CL (4.08 g, 35.75 mmol) were charged to a 50 mL round-bottom flask equipped with a dry magnetic stirring bar, and Sn(Oct)<sub>2</sub> [1/1000 (wt) with respect to  $\epsilon$ -CL] was added. The flask was connected to a standard Schlenk line, and the reactive mixture was degassed *via* three pump-freeze-thaw cycles and then immersed in a thermostated oil bath at 120 °C for 36 h. The crude product was dissolved in tetrahydrofuran, and the solution was

dropped into an excessive amount of petroleum ether to afford the white precipitates. Then the product was dried in a vacuum oven for 40 h with a yield of 98% (3.99 g). The molecular weight was determined to be  $M_n = 3650$  according to the ratio of integral intensity of the near-end methylene protons (at  $\delta = 3.65$  ppm in  $\text{CDCl}_3$ ) to that of the methylene protons of polymeric structure (e.g., the methylene connected to carbonyl groups at  $\delta = 2.1$  or 4.0 ppm) in its  $^1\text{H-NMR}$  spectrum.

## 2.5. Preparation of epoxy thermosets containing triblock copolymer

The PCL-*b*-PEEE-*b*-PCL triblock copolymer was added to DGEBA with continuous stirring at 100 °C until the mixtures became homogenous and transparent and then 4,4'-methylenebis(2-chloroaniline) was added with continuous stirring until the full dissolution of the curing agent. The mixtures were poured into Teflon molds and cured at 150 °C for 2 h plus 180 °C for 2 h. The thermosets containing the block copolymer up to 40 wt % were obtained.

## 2.6. Measurements and characterization

### 2.6.1. Fourier transform infrared spectroscopy (FTIR)

The FTIR measurements were conducted on a Perkin Elmer Spectrum 100 Fourier transform infrared spectrometer at room temperature (25 °C). The block copolymer (0.1 g) was dissolved in 20 ml anhydrous toluene and then the solution of the diblock copolymer was cast onto KBr windows at 60 °C and the residual solvent was removed *in vacuo* at 60 °C for 1 h. The specimens of thermosets were granulated and the powder was mixed with KBr pellets to press into the small flakes. All the specimens were sufficiently thin to be within a range where the Beer–Lambert law is obeyed. In all cases 64 scans at a resolution of  $2\text{ cm}^{-1}$  were used to record the spectra.

### 2.6.2. Nuclear magnetic resonance spectroscopy (NMR)

The NMR measurements were carried out on a Varian Mercury Plus 400 MHz nuclear magnetic resonance spectrometer. The hydroxyl-terminated polybutadiene and poly(ethylene-*co*-ethyl-ethylene) were dissolved with deuterium chloroform and benzene, respectively; the  $^1\text{H-NMR}$  spectra were obtained with tetramethylsilane (TMS) as the internal reference.

### 2.6.3. Atomic force microscopy (AFM)

The specimens of thermosets for AFM observation were trimmed using a microtome machine, and the thickness of the specimens was about 70 nm. The morphological observation of the specimens was conducted on a Nanoscope IIIa scanning probe microscope (Digital Instruments, Santa Barbara, CA) in tapping mode. A tip fabricated from silicon (125  $\mu\text{m}$  in length with *c.a.* 500 kHz resonant frequency) was used for scan, and the scan rate was 2.0 Hz.

### 2.6.4. Dynamic mechanical thermal analysis (DMTA)

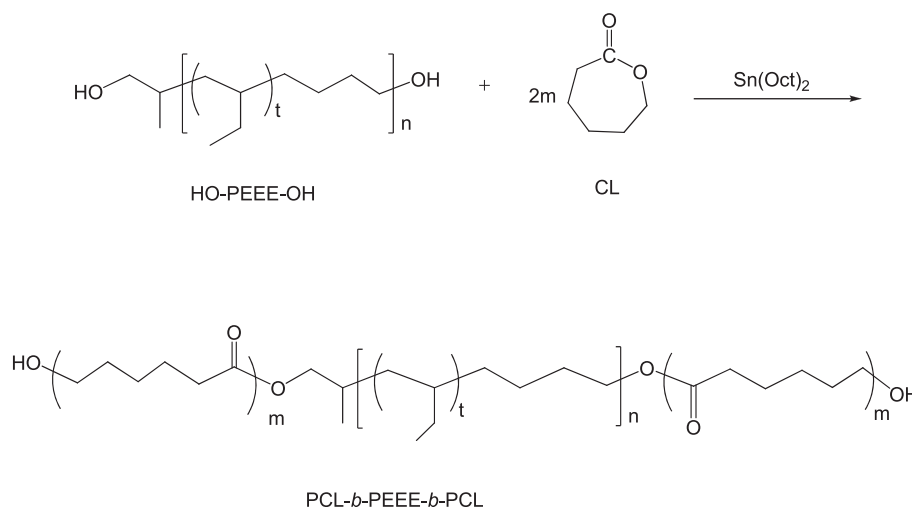
The dynamic mechanical tests were carried out on a TA Instruments DMA Q800 dynamic mechanical thermal analyzer (DMTA) equipped with a liquid nitrogen apparatus in a single cantilever mode. The frequency used is 1.0 Hz and the heating rate 3.0 °C/min. The specimen dimension was  $25 \times 5.0 \times 1.75\text{ mm}^3$ . The experiments were carried out from  $-100\text{ °C}$  until the samples became too soft to be tested.

### 2.6.5. Differential scanning calorimetry (DSC)

Thermal analysis was performed on a Perkin Elmer Pyris-1 differential scanning calorimeter in a dry nitrogen atmosphere. The instrument was calibrated with a standard Indium. The samples (about 10.0 mg in weight) were first heated up to 200 °C and held at this temperature for 3 min to eliminate thermal history, followed by quenching to  $-70\text{ °C}$ . To measure glass transition temperatures ( $T_g$ ), a heating rate of 20 °C/min was used in all cases and glass transition temperature ( $T_g$ ) was taken as the midpoint of the heat capacity change and the melting point ( $T_m$ ) was taken as the temperature at the maximum of endothermic transition. For a cooling scan, the cooling rate of 10 °C/min was used and the minima of exothermic peaks were taken as the temperatures of crystallization ( $T_c$ ).

### 2.6.6. Small-angle X-ray scattering (SAXS)

The SAXS measurements were taken on a Bruker Nanostar system. Two-dimensional diffraction patterns were recorded using an image intensified CCD detector. The experiments were carried out at room temperature (25 °C) using Cu K $\alpha$  radiation ( $\lambda = 1.54\text{ \AA}$ , wavelength) operating at 40 kV, 35 mA. The intensity profiles were output as the plot of scattering intensity ( $I$ ) versus scattering vector,  $q = (4\pi/\lambda) \sin(\theta/2)$  ( $\theta =$  scattering angle). The variable temperature measurements of SAXS were carried out on a small-angle X-ray scattering station (BL16B1) of Shanghai Synchrotron Radiation



**Scheme 1.** Synthesis of PCL-*b*-PEEE-*b*-PCL triblock copolymer.

Facility (SSRF), Shanghai, China, in which the third generation of synchrotron radiation light source was employed. Two-dimensional diffraction patterns were recorded using an image intensified CCD detector. The experiments were carried out with the radiation of X-ray with the wavelength of  $\lambda = 1.24 \text{ \AA}$ . A TH MS600 Linkam hotstage with the precision of  $0.1 \text{ }^\circ\text{C}$  was mounted and used for the experiments of variable temperatures. The intensity profiles were output as the plot of scattering intensity (I) versus scattering vector,  $q = (4\pi/\lambda) \sin(\theta/2)$  ( $\theta =$  scattering angle).

### 3. Results and discussion

#### 3.1. Synthesis of triblock copolymers

The route of synthesis for poly( $\epsilon$ -caprolactone)-*block*-poly(ethylene-*co*-ethylethylene)-*block*-poly( $\epsilon$ -caprolactone) (PCL-*b*-PEEE-*b*-PCL) triblock copolymer is shown in Scheme 1. The ring-opening polymerization of  $\epsilon$ -caprolactone with a hydroxyl-terminated poly(ethylene-*co*-ethylethylene) as the macromolecular initiator was carried out with stannous octanoate [Sn(Oct)<sub>2</sub>] as the catalyst. The hydroxyl-terminated poly(ethylene-*co*-ethylethylene) was prepared *via* the hydrogenation of a hydroxyl-terminated polybutadiene with tosylhydrazide as a reducing agent [38–41] (Scheme 2). The reaction of reduction was carried out in the solution of xylene at  $120 \text{ }^\circ\text{C}$  for 15 h and the degree of hydrogenation was traced by means of Fourier transform infrared spectroscopy (FTIR). Shown in Fig. 1 are the FTIR spectra of both hydroxyl-terminated polybutadiene and hydroxyl-terminated poly(ethylene-*co*-ethylethylene). For the hydroxyl-terminated polybutadiene, the broad band at  $3432 \text{ cm}^{-1}$  is ascribed to the stretching vibration of terminal hydroxyl groups; the C=C double bonds in polybutadiene were characterized by two bands at  $3078$  and  $1641 \text{ cm}^{-1}$ , respectively. The former is assignable to the stretching vibration of C–H bonds in unsaturated moiety (C=C) whereas the latter is ascribed to the stretching vibration of C=C double bonds in unconjugated alkene. With the occurrence of the hydrogenation, it is noted that these two bands were virtually depleted and instead an intense band characteristic of the deformation vibration of alkyl methylene appeared at  $1462 \text{ cm}^{-1}$ , indicating that the reaction of reduction was performed to completion (See Curve B in Fig. 1). It is seen that the stretching vibration of hydroxyl groups at  $3432 \text{ cm}^{-1}$  of the reduced product was still detected at  $3432 \text{ cm}^{-1}$ , implying that the hydroxyl groups remained unchanged by the reaction of hydrogenation. The <sup>1</sup>H-NMR spectra of the hydroxyl-terminated polybutadiene and poly(ethylene-*co*-ethylethylene) were presented in Fig. 2. For the former, the resonance at 1.2–1.4 ppm is assignable to the protons of main-chain methylene in the 1,2 structure of polybutadiene whereas the resonance at 1.8–2.2 ppm to the protons of main-chain methine in the 1,2 structure of polybutadiene [*i.e.*, (CH<sub>2</sub>=CH)CHCH<sub>2</sub> in 1,2 structure]. The intense signal at 2.0–2.2 ppm is attributed to the resonance of the protons of methylene groups in 1,4 structure of polybutadiene (*i.e.*, CH<sub>2</sub>CH=CHCH<sub>2</sub> in 1,4 structure). The peaks at 4.8–5.0 ppm are ascribed to the resonance of the protons connected to the double bonds in 1,2 structure of polybutadiene [*i.e.*, –CH=CH<sub>2</sub> in 1,2 structure] whereas those at 5.3–5.5 ppm to the resonance of the protons connected to the double bonds in 1,4 structure of polybutadiene

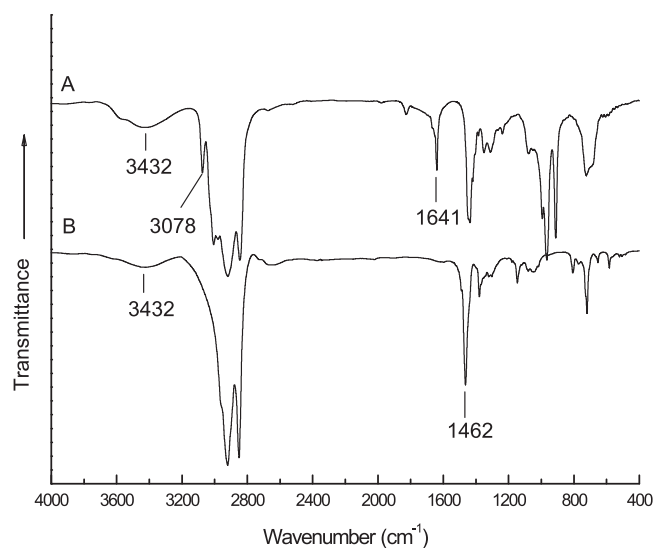
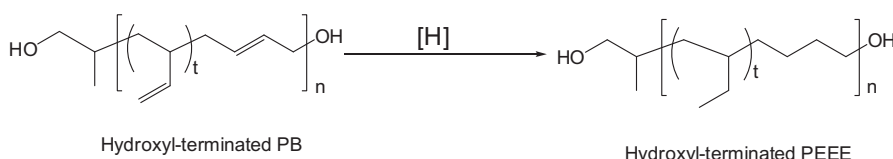


Fig. 1. FTIR spectra of hydroxyl-terminated polybutadiene (A) and poly(ethylene-*co*-ethylethylene) (B).

[*i.e.*, H<sub>2</sub>CCH=CHCH<sub>2</sub> in 1,4 structure]. With the occurrence of hydrogenation, all the signals assignable to the protons connected to C=C double bonds vanished, indicating that the reaction of hydrogenation has been carried out to completion. It is seen that the signals at 0.91 and 1.33 ppm appeared after the hydroxyl-terminated polybutadiene was hydrogenated. The former is ascribed to the resonance of methyl protons whereas the latter to the combined resonance of methylene and methine groups. The resonance at 3.31 ppm is ascribed to the protons of methylene connected to the terminal hydroxyl groups, which can be used to estimate the molecular weight of the hydroxyl-terminated poly(ethylene-*co*-ethylethylene). The FTIR and <sup>1</sup>H-NMR spectroscopy indicates that the hydroxyl-terminated polybutadiene has been completely hydrogenated, *i.e.*, the hydroxyl-terminated poly(ethylene-*co*-ethylethylene) was successfully obtained.

The above hydroxyl-terminated poly(ethylene-*co*-ethylethylene) was used as the macromolecular initiator to synthesize poly( $\epsilon$ -caprolactone)-*block*-poly(ethylene-*co*-ethylethylene)-*block*-poly( $\epsilon$ -caprolactone) (PCL-*b*-PEEE-*b*-PCL) triblock copolymer *via* the ring-opening polymerization of  $\epsilon$ -caprolactone with stannous octanoate [Sn(Oct)<sub>2</sub>] as the catalyst. The <sup>1</sup>H-NMR spectrum of PCL-*b*-PEEE-*b*-PCL triblock copolymer is shown in Fig. 3. The signals of resonance for PCL blocks were detected at 1.38, 1.63, 2.31 and 4.06 ppm, which are assignable to the protons of methylene of PCL chains as indicated in the spectrum. The resonance at 0.91 ppm is discernable, indicating the presence of PEEE blocks. The length of PCL block in the triblock copolymer can be estimated to 3650 Da according to the ratio of the integral intensity for the protons connected to the terminal hydroxyl groups at 3.31 ppm to that of other methylene in the PCL chains, *i.e.*, the molecular weight of PCL-*b*-PEEE-*b*-PCL triblock copolymer is calculated to be *c.a.*  $M_n = 10,900$ . The PCL-*b*-PEEE-*b*-PCL triblock copolymer was



Scheme 2. Hydrogenation of a hydroxyl-terminated polybutadiene.

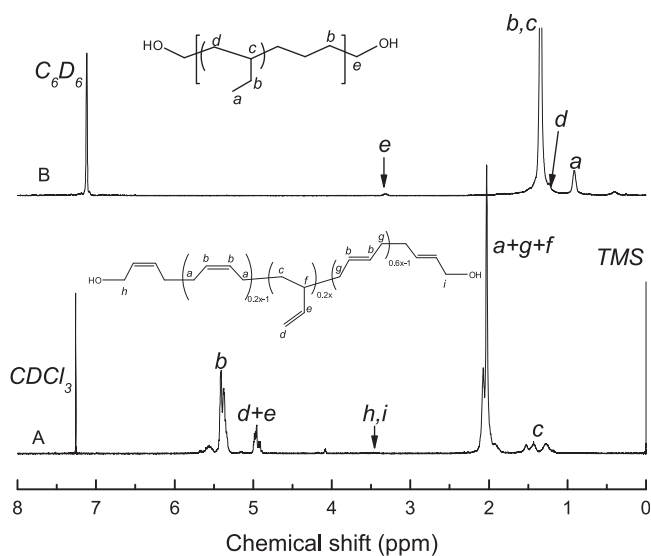


Fig. 2. <sup>1</sup>H-NMR spectra of (A) hydroxyl-terminated polybutadiene, (B) poly(ethylene-co-ethylene).

subjected to differential scanning calorimetry (DSC) and the DSC curves are presented in Fig. 4. In the heating scan, two endothermic peaks were exhibited at 56 and 74 °C, respectively (See curve A). The former is assignable to the melting transition of PCL blocks whereas the latter to that of PEEE blocks. This observation was further confirmed with the cooling scan (See curve B). It is seen that two exothermic peaks were detected at 41 and 26 °C, which are ascribed to the crystallization of PEEE and PCL blocks, respectively. The results of DSC indicate that the triblock copolymer contains two crystallizable blocks, *i.e.*, PCL and PEEE.

### 3.2. Nanostructured epoxy thermosets

The PCL-*b*-PEEE-*b*-PCL triblock copolymer was incorporated into epoxy to prepare the thermosets. Before curing, all the mixtures composed of DGEBA, MOCA and PCL-*b*-PEEE-*b*-PCL triblock copolymer are homogenous and transparent, indicating that no macroscopic phase separation occurred at the scale exceeding the wavelength of visible light. The reactive mixtures were cured at 150 °C for 2 h plus 180 °C for 2 h to obtain the thermosets. All the as-prepared thermosets were homogenous and transparent, indicating

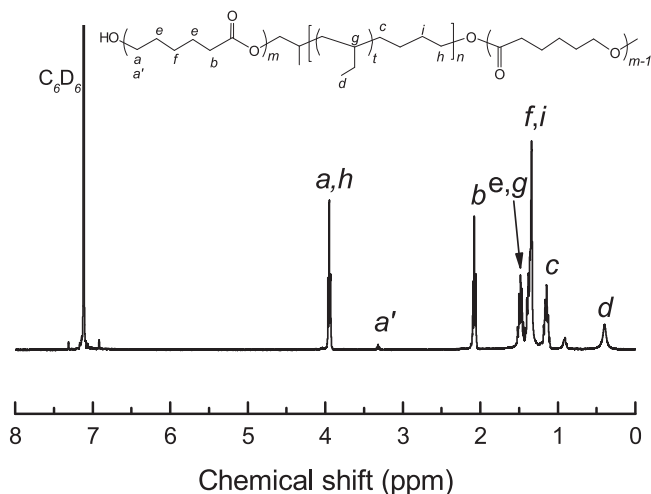


Fig. 3. <sup>1</sup>H-NMR spectrum of PCL-*b*-PEEE-*b*-PCL triblock copolymer.

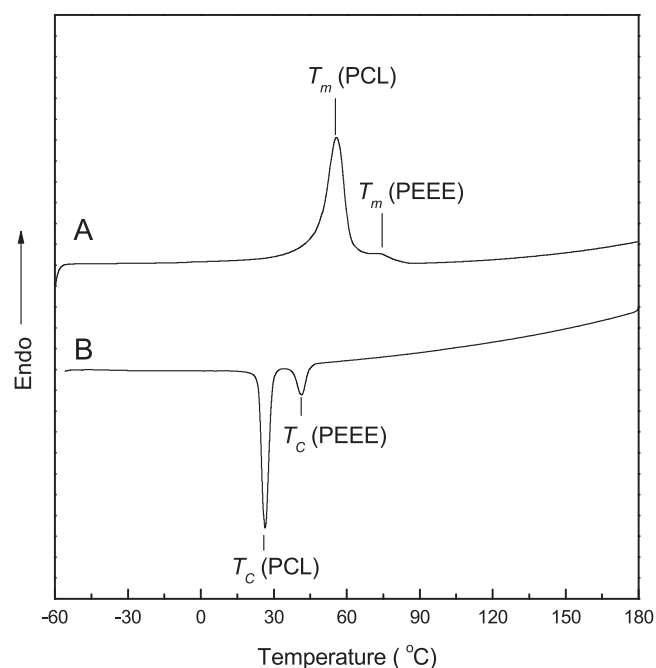


Fig. 4. DSC curves of PCL-*b*-PEEE-*b*-PCL triblock copolymer: A) a heating scan at the rate of 20 °C/min, B) a cooling scan at the rate of 10 °C/min.

that no macroscopic phase separation occurred in the resulting thermosets. The epoxy thermosets containing PCL-*b*-PEEE-*b*-PCL triblock copolymer were subjected to the morphological observation by means of atomic force microscopy (AFM) and small-angle X-ray scattering (SAXS).

Shown in Fig. 5 are the AFM micrographs of the thermosets containing 10, 20, 30 and 40 wt% PCL-*b*-PEEE-*b*-PCL triblock copolymer. The left and right images are the topography and phase contrast images, respectively. It is seen that the microphase-separated morphologies were exhibited in all the cases. In terms of the volume fraction of the block copolymer and the difference in viscoelastic properties between epoxy matrix and the subchains of triblock copolymer, the dispersed nanodomains are assignable to the immiscible components (*i.e.*, PEEE) whereas the continuous matrix to epoxy, which was miscible with PCL subchains. For the thermosets containing 10 and 20 wt% PCL-*b*-PEEE-*b*-PCL triblock copolymer, the spherical particles with the size of 10–20 nm in diameter were dispersed into continuous matrix (Fig. 5 A and B). With increasing the content of PCL-*b*-PEEE-*b*-PCL triblock copolymer the separate PEEE nanodomains gradually became interconnected. While the content of PCL-*b*-PEEE-*b*-PCL triblock copolymer is 30 wt% or more, worm-like nanodomains appeared (Fig. 5 C and D). The morphologies of the thermosets were further investigated by small-angle X-ray scattering (SAXS) and the SAXS profiles are presented in Fig. 6. In all the cases, the well-defined scattering peaks at  $q \approx 0.25 \text{ nm}^{-1}$  were displayed, indicating that the thermosets containing the triblock copolymer are microphase-separated. It is seen that the scattering vectors shifted to the lower values with increasing the content of the triblock copolymer. According to the positions of the primary scattering peaks, the principal domain spacing  $d_m$ 's were calculated, which can be taken as the measures of the average distance of adjacent microdomains. The principal domain spacing  $d_m$ 's were obtained to be 23.6, 22.3, 20.5 and 19.7 nm for the thermosets containing 10, 20, 30 and 40 wt % of PCL-*b*-PEEE-*b*-PCL diblock copolymer, respectively. This result is in a good agreement with those obtained by means of AFM.

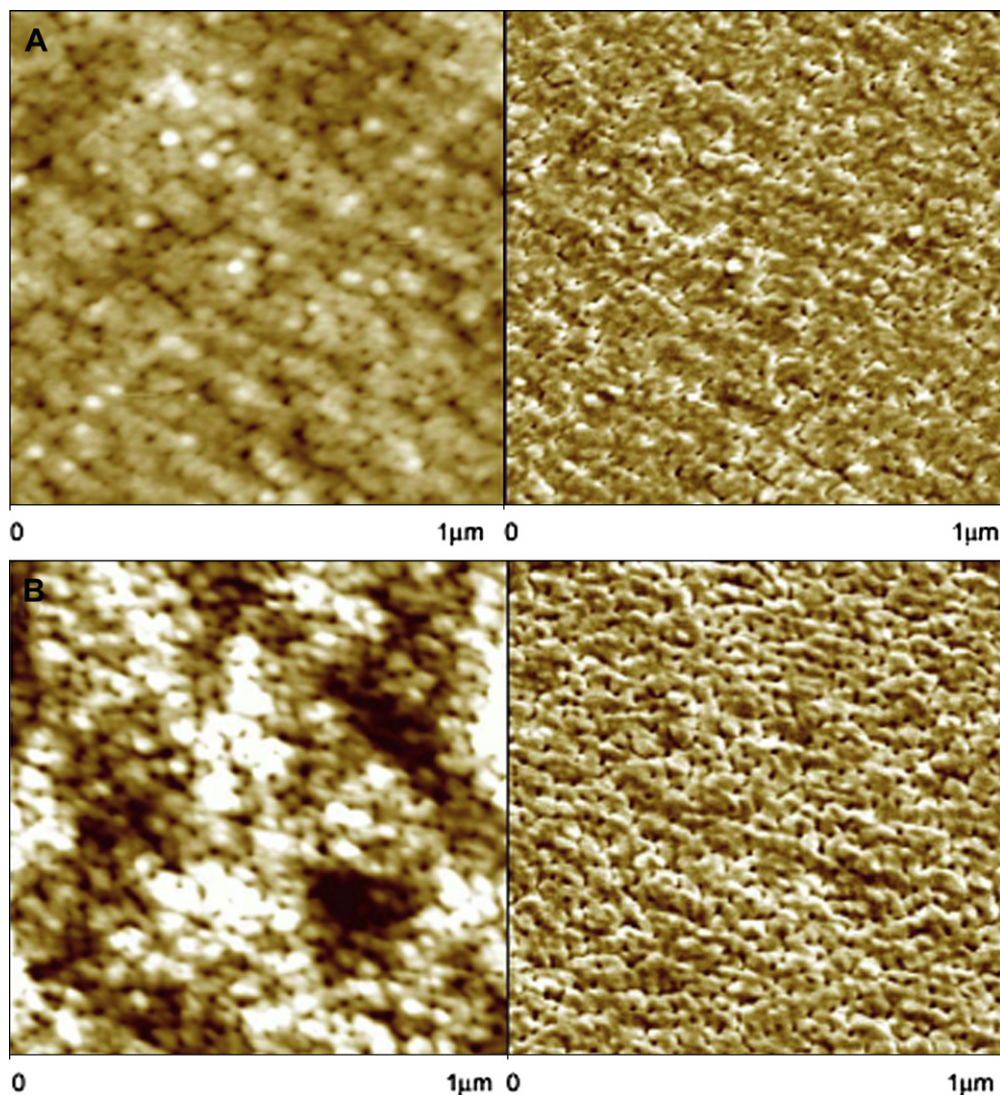


Fig. 5. AFM images of the thermosets containing: (A) 10, (B) 20, (C) 30 and (D) 40wt % of PCL-*b*-PEEE-*b*-PCL triblock copolymer. Left: topography. Right: phase contrast images.

### 3.3. Self-assembly behavior of PCL-*b*-PEEE-*b*-PCL in epoxy resin

In a previous work [26], we have demonstrated that the formation of the nanostructures in epoxy thermosets containing poly( $\epsilon$ -caprolactone)-*block*-polybutadiene-*block*-poly( $\epsilon$ -caprolactone) triblock copolymer (PCL-*b*-PB-*b*-PCL) followed the mechanism of reaction-induced microphase separation. At the beginning of the curing reaction, all the subchains (*viz.* PB and PCL) of the triblock copolymer were miscible with the precursors (*viz.* DGEBA and MOCA) at the curing temperature (*viz.* 150 °C), *i.e.*, no pre-formed self-assembly structures were formed at the beginning of curing reaction. With the curing reaction proceeding, the PB subchains were microphase-separated out from epoxy matrix whereas the PCL subchains remained miscible with the epoxy networks. In the present case, the midblock of the triblock copolymer has been converted into poly(ethylene-co-ethylethylene) (PEEE) *via* the hydrogenation of PB. Owing to the change in solubility parameters resulting from the hydrogenation, the formation of the nanostructures in epoxy thermosets containing PCL-*b*-PEEE-*b*-PCL triblock copolymer would follow a quite different mechanism. In fact, it was observed that the hydrogenated hydroxyl-terminated PB (*viz.* the hydroxyl-terminated PEEE) was no longer miscible with epoxy

precursors (*i.e.*, DGEBA + MOCA) at either room temperature or 150 °C, which was in marked contrast to the hydroxyl-terminated PB [26]. This observation suggests that the PCL-*b*-PEEE-*b*-PCL triblock copolymer would be self-organized into the nanophases in the precursors of epoxy resin. The self-assembly behavior was readily investigated by means of small-angle X-ray scattering (SAXS). The SAXS measurements were carried out at 80 °C and 150 °C, respectively. The former is above the melting temperature of PEEE (and/or PCL) blocks to melt the crystals of PEEE (and/or PCL) blocks whereas the latter corresponds to the curing temperature used in this work. Shown in Fig. 7 are the SAXS profiles of the ternary mixture of DGEBA, MOCA and PCL-*b*-PEEE-*b*-PCL, in which the fraction of the triblock copolymer was 20 wt%. The mixture displayed a scattering peak at  $q = 0.19 \text{ nm}^{-1}$  at 80 °C, indicating that the mixture was microphase-separated, *i.e.*, the PCL-*b*-PEEE-*b*-PCL triblock copolymer was self-organized into the nanophases in the mixture. In term of the  $q$  value of scattering peak the principal spacing is calculated to be  $d_m = 31.4 \text{ nm}$ . While the mixture was heated up to the curing temperature (*i.e.*, 150 °C) the scattering peak still existed, suggesting that the self-organized nanophases were reserved at the beginning of curing reaction. The SAXS results indicate that the formation of the nanostructures in epoxy thermosets containing

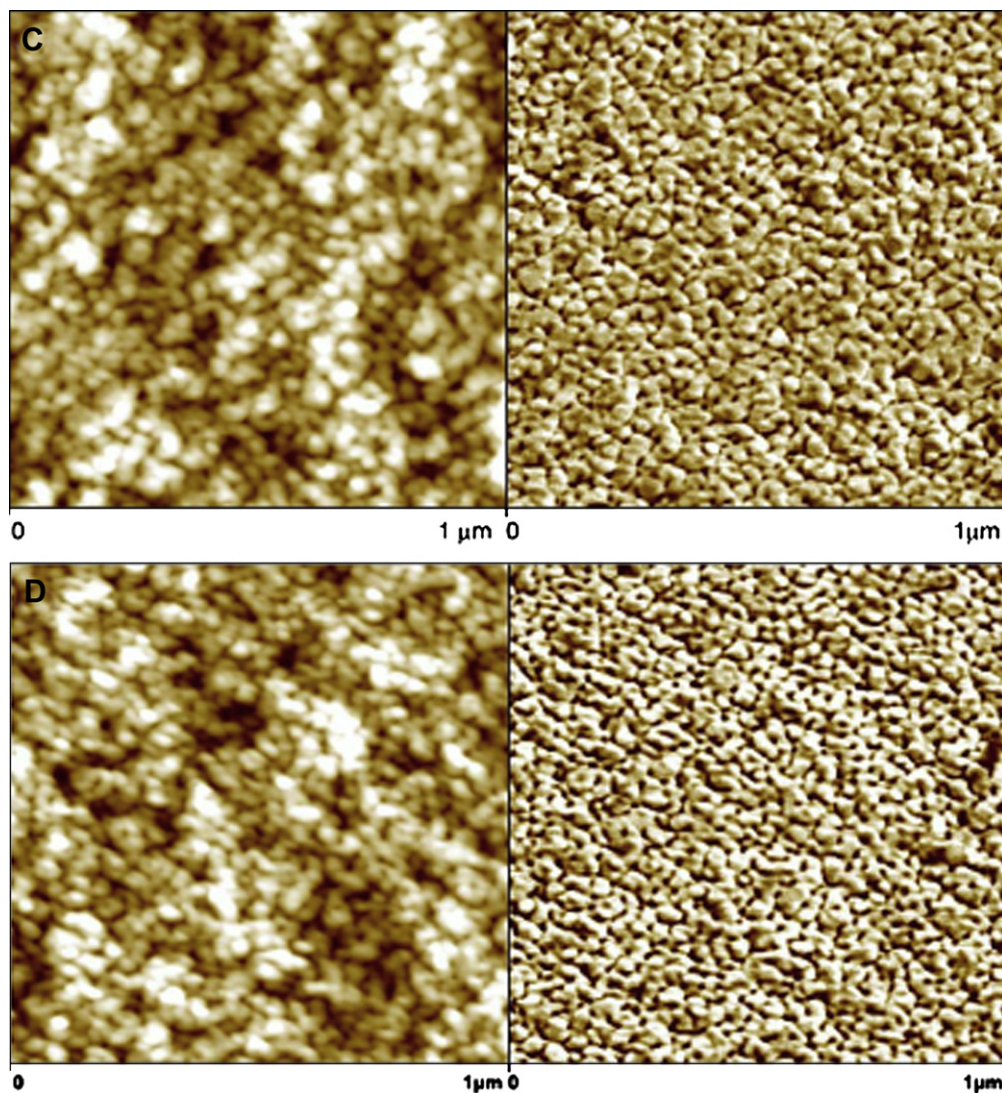


Fig. 5. (continued).

PCL-*b*-PEEE-*b*-PCL triblock copolymer followed self-assembly mechanism. It should be pointed out that the principal spacing of  $d_m = 31.4$  nm before the curing reaction was much higher than that ( $d_m = 22.3$  nm) of the thermoset containing 20 wt% PCL-*b*-PEEE-*b*-PCL triblock copolymer. The decreased average distance between two adjacent PEEE microdomains could be ascribed to the demixing behavior of PCL subchains due to the occurrence of the curing reaction.

It is proposed that in the nanostructured thermosets the PEEE blocks were microphase-separated whereas the PCL blocks were miscible with epoxy thermosets. The miscibility of PCL with the epoxy matrix can be investigated by glass transition behavior of the nanostructured thermosets. In this work, the thermosets containing PCL-*b*-PEEE-*b*-PCL were subjected to dynamic mechanical thermal analysis (DMTA). Shown in Fig. 8 are the dynamic mechanical spectra of the nanostructured thermosets. The control epoxy exhibited a well-defined relaxation peak (*i.e.*,  $\alpha$  transition) centered at *c.a.* 159 °C, which is responsible for the glass–rubber transition of the crosslinked polymer. Apart from the  $\alpha$  transition, the MOCA-cured epoxy exhibited a secondary transition (*viz.*  $\beta$ -relaxation) at the lower temperature ( $\sim -60$  °C). This transition is attributed predominantly to the motion of hydroxyl ether structural units

[–CH<sub>2</sub>–CH(OH)–CH<sub>2</sub>–O–] and diphenyl groups in amine-cross-linked epoxy [42–44]. It is seen that upon adding PCL-*b*-PEEE-*b*-PCL triblock copolymer into the thermosets, the  $\alpha$  transition shifted to the lower temperatures. The  $T_g$ 's decreased with increasing the content of the triblock copolymer diblock copolymer. The decreased  $T_g$ 's are ascribed to the plasticization of PCL subchains of the block copolymer on the epoxy matrix. For the nanostructured thermoset containing 40 wt% PCL-*b*-PEEE-*b*-PCL, a new transition appeared at  $-40$  °C. The new peak could be assigned to the glass transition of the PEEE microdomains in the nanostructured thermosets. It should be pointed out that while the content of PCL-*b*-PEEE-*b*-PCL triblock copolymer is less than 40 wt% this peak was not discernible due possibly to too low content of amorphous PEEE because PEEE is crystalline.

The miscibility of PCL block with epoxy matrix is responsible for the formation of the intermolecular hydrogen bonding interactions between the PCL block and epoxy matrix, which is readily evidenced by Fourier transform infrared spectroscopy (FTIR). In Fig. 9, the FTIR spectra of PCL-*b*-PEEE-*b*-PCL triblock copolymer and the nanostructured epoxy thermosets were presented in the range of 1640–1800  $\text{cm}^{-1}$ . These bands are ascribed to the stretching vibration of carbonyl groups. For PCL-*b*-PEEE-*b*-PCL triblock

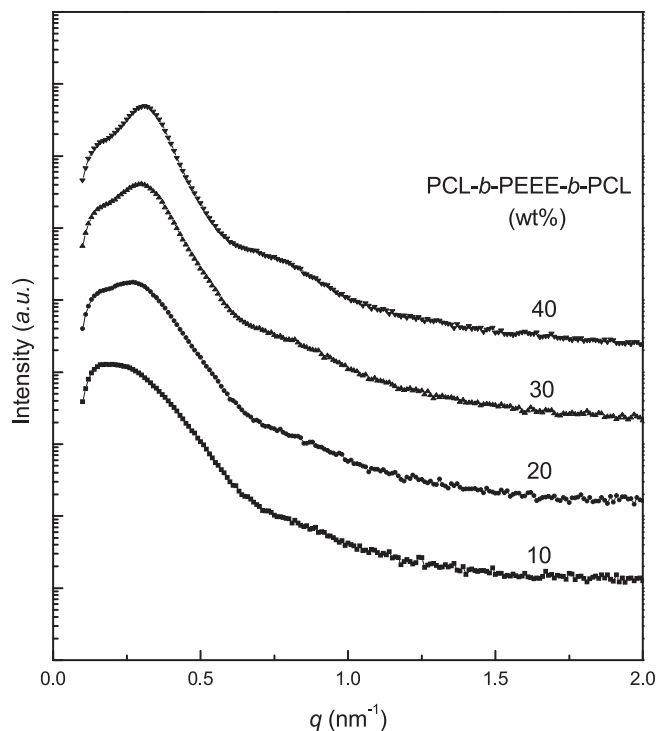


Fig. 6. SAXS profiles of the nanostructured thermosets containing PCL-*b*-PEEE-*b*-PCL triblock copolymers at 80 °C.

copolymer, the band is composed of two components at 1735 and 1725  $\text{cm}^{-1}$ , respectively, which are sensitive to the conformation of PCL chain. The former is attributed to the carbonyl groups of PCL in amorphous region whereas the latter to those in crystalline region [45,46]. When this triblock copolymer was incorporated into epoxy thermosets it is seen that the component at 1725  $\text{cm}^{-1}$  disappeared; instead the new shoulder band at 1710  $\text{cm}^{-1}$  appeared. In addition,

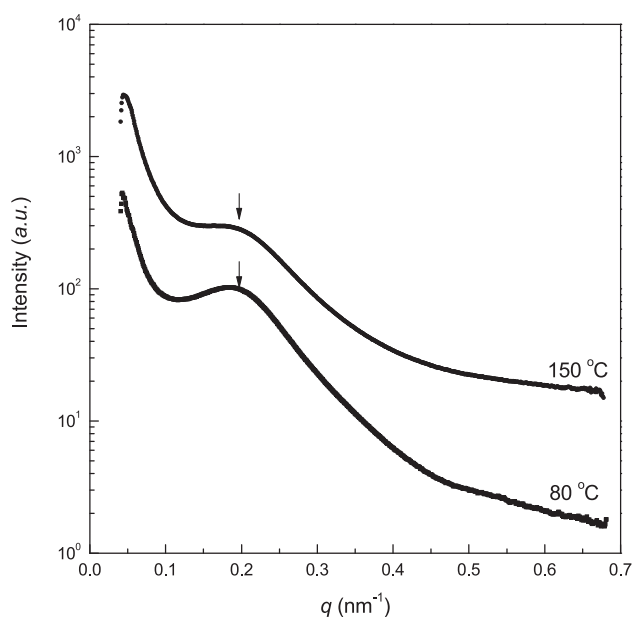


Fig. 7. SAXS profiles of the mixture containing 80 wt% of epoxy precursors (viz. DGBBA + MOCA) and 20 wt% of PCL-*b*-PEEE-*b*-PCL triblock copolymer at 80 °C and 150 °C.

the band at 1735  $\text{cm}^{-1}$  was observed to shift to lower frequency (*i.e.*, 1732  $\text{cm}^{-1}$ ). The disappearance of the shoulder at 1725  $\text{cm}^{-1}$  indicates that the PCL blocks were no longer crystalline due to the miscibility between the aromatic amine-cured epoxy and PCL [47,48]. The new shoulder bands at 1710  $\text{cm}^{-1}$  are ascribed to the stretching vibration of the hydrogen-bonded carbonyl groups. The FTIR results indicate that the intermolecular hydrogen bonding interactions between carbonyl groups of PCL and hydroxyl groups of crosslinked epoxy networks were formed in the nanostructured thermosets.

### 3.4. Demixing behavior of PCL subchains

In terms of DMTA and FTIR spectroscopy, it is judged that the PCL blocks were mixed with epoxy matrix whereas PEEE blocks were microphase-separated. Nonetheless, the mixing degree of PCL blocks with the epoxy matrix could be affected by the formation of microphase-separated morphology. By means of SAXS, Hillmyer et al. [3,4] investigated the demixing of poly(ethylene oxide) block in the nanostructured epoxy thermosets containing poly(ethylene oxide)-*block*-poly(ethyl ethylene) diblock copolymer. In the present work, the demixing behavior of PCL blocks was investigated by means of differential scanning calorimetry (DSC). The DSC curves of control epoxy and the nanostructured thermosets containing the triblock copolymer are shown in Fig. 10. Each nanostructured thermoset displayed a glass transition in the range of 60–160 °C depending on the content of PCL-*b*-PEEE-*b*-PCL, which is assignable to the epoxy matrix containing PCL subchains. It is seen that the  $T_g$ 's decreased with increasing the content of PCL-*b*-PEEE-*b*-PCL triblock copolymer. Apart from the glass transition, a melting peak at *c.a.* 73 °C was exhibited in the DSC curve of each nanostructured thermoset and the intensity of the melting peak increased with increasing the content of the triblock copolymer. The melting peaks are ascribed to the fusion of PEEE blocks. The fact that the melting transition of PEEE blocks appeared prior to the glass transition of epoxy matrix indicates that PEEE blocks were microphase-separated, *i.e.*, the PEEE subchains existed in the thermosets in the form of microdomains. In the DSC measurements the glass transition of PEEE microdomains was not sufficiently strong to be detected, nonetheless, the results of DMTA measurement gave a  $T_g$  of –41 °C for the PEEE microdomain while the content of PCL-*b*-PEEE-*b*-PCL triblock copolymer is 40 wt% (See Fig. 8). It should be pointed out that the melting transition is not assigned to the melting transition of PCL since the PCL blocks were not crystalline in the nanostructured thermosets.

The  $T_g$  values of epoxy matrix containing PCL blocks can be employed to evaluate the mixing degree of PCL blocks in epoxy thermosets. There are several theoretical and empirical equations to account for the dependence of  $T_g$  on composition in miscible polymer blends [49–51]. Of them Couchman equation [51] is frequently used:

$$\ln T_g = [W_1 k \ln T_{g1} + W_2 \ln T_{g2}] / (W_1 k + W_2) \quad (1)$$

where  $W_i$  is the weight fraction of component  $i$  and  $T_{g_i}$  is the glass transition temperature of blend; the parameter  $k$  is Couchman coefficient defined by:

$$k = \Delta C_{p1} / \Delta C_{p2} \quad (2)$$

where  $\Delta C_{p_i}$  designates the increment of the heat capacity of the specimen at glass transition. In this work, we prepared the binary blends of epoxy thermoset with the model PCL having the identical molecular weight with the length of PCL block in the triblock copolymer since the binary blends of epoxy with PCL have been demonstrated to be miscible over the entire composition [47,48].



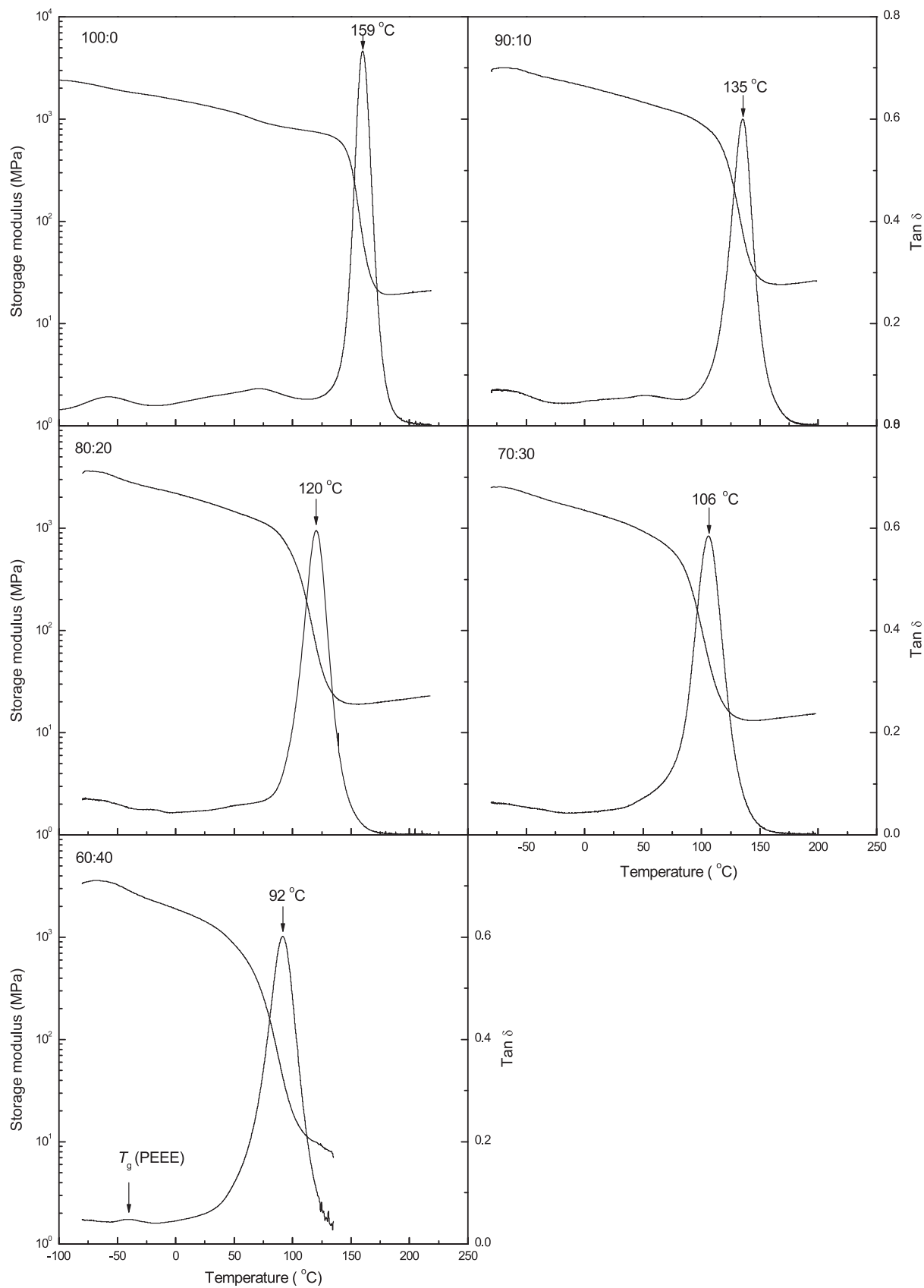


Fig. 8. DMTA curves of the binary blends of epoxy resin containing PCL-*b*-PEEE-*b*-PCL triblock copolymer.

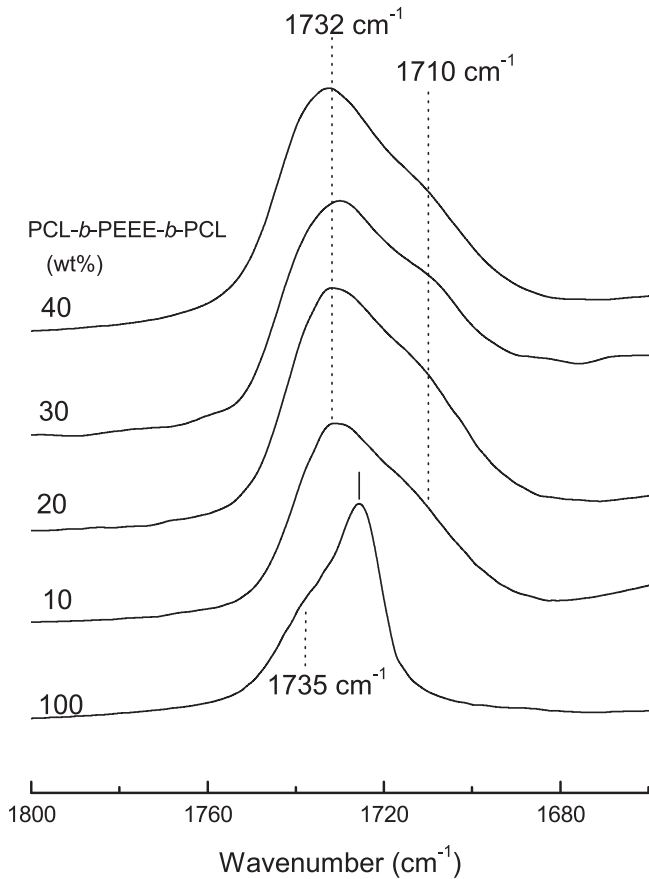


Fig. 9. FTIR spectra of PCL-*b*-PEEE-*b*-PCL triblock copolymer and the nanostructured epoxy thermosets.

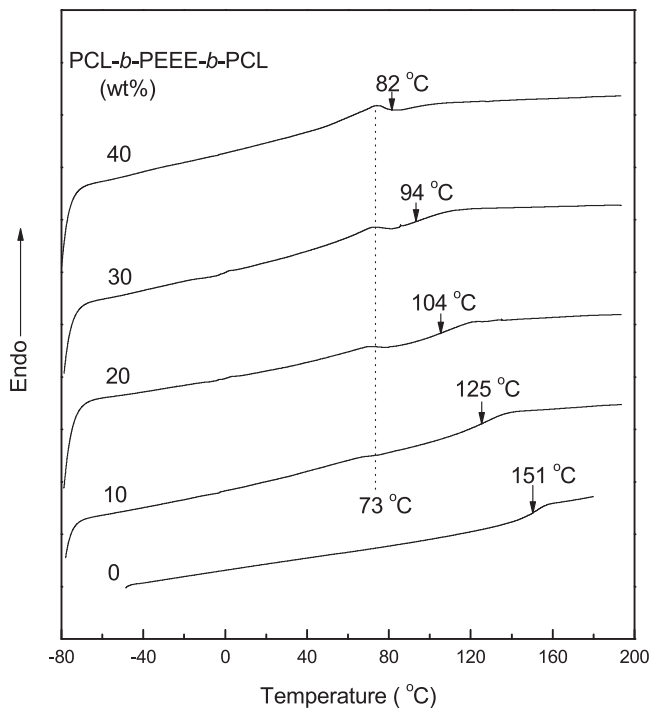


Fig. 10. DSC curves of the nanostructured thermosets containing PCL-*b*-PEEE-*b*-PCL triblock copolymer.

The value of  $k$  was determined to be 1.34 (the DSC curves not shown here for brevity) (See Fig. 11). Under the identical condition, the thermal analyses were also carried out for the nanostructured epoxy thermosets containing the PCL-*b*-PEEE-*b*-PCL triblock copolymers. The plots of  $T_g$ 's as functions of the concentration of PCL for the nanostructured thermosets are also incorporated in Fig. 11. It should be pointed out that the concentration of PCL in the thermosetting matrix has been re-calculated by deducting the fraction of PEEE block according to the composition of the triblock copolymer. It is noted that at the identical content of PCL block in the epoxy blends, the nanostructured thermosets containing 30 and 40 wt% PCL-*b*-PEEE-*b*-PCL triblock copolymer (which correspond to 21.7 and 31.5 wt% PCL in the thermosetting matrices) displayed higher  $T_g$ 's than the binary blends of epoxy with the model PCL with the identical contents of PCL. The enhanced  $T_g$ 's resulted from the demixing of PCL subchains owing to the formation of the nanostructures in the thermosets. In the binary thermosetting blends, the PCL chains were homogeneously dispersed into the epoxy matrix and were well interpenetrated into the crosslinked epoxy networks *via* the formation of the intermolecular hydrogen bonding interactions. In contrast, the PCL chains have to be enriched at the surfaces of the microphase-separated PEEE nanodomains due to the presence of chemical bonds between PEEE and PCL blocks in the nanocomposites. Due to the steric hindrance, the PCL chains at the intimate surface of PEEE microdomains could not be well mixed with epoxy matrix and thus the less PCL chains were miscible with the epoxy matrix, *i.e.*, the plasticization of PCL chains on the epoxy matrix would be effectively weakened, which caused the increased  $T_g$ 's of epoxy matrix. The quantity of demixed PCL can be readily estimated according to the  $T_g$ -composition curve of the binary blends of epoxy with the model PCL and the experimental  $T_g$ 's of the nanostructured thermosets. For instance, the fractions of demixed PCL subchains were *c.a.* 27.5 and 33.4 wt% for the nanostructured thermosets containing 30 and 40 wt% PCL-*b*-PEEE-*b*-PCL triblock copolymer, respectively.

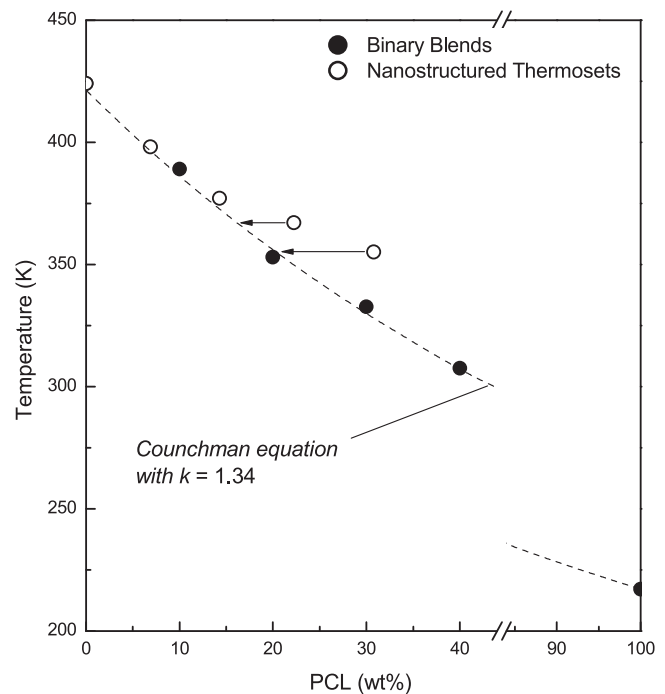


Fig. 11. Plots of  $T_g$ 's as functions of concentration of PCL for epoxy thermosets containing the block copolymers.

#### 4. Conclusions

Poly( $\epsilon$ -caprolactone)-*block*-poly(ethylene-*co*-ethylethylene)-*block*-poly( $\epsilon$ -caprolactone) triblock copolymer was synthesized by the ring-opening polymerization of  $\epsilon$ -caprolactone with a hydroxyl-terminated poly(ethylene-*co*-ethylethylene) as the initiator. The hydroxyl-terminated poly(ethylene-*co*-ethylethylene) was prepared through the hydrogenation of a hydroxyl-terminated polybutadiene and it was characterized by means of Fourier transform infrared spectroscopy (FTIR), nuclear magnetic resonance spectroscopy (NMR) and differential scanning calorimetry (DSC). The triblock copolymer was incorporated into epoxy resin and the self-organized nanostructures were formed before curing reaction as evidenced by small-angle X-ray scattering. The nano-phases in epoxy were further fixed by initiating the curing reaction of epoxy resin. Atomic force microscopy (AFM) and small-angle X-ray scattering (SAXS) showed that poly(ethylene-*co*-ethylethylene) was dispersed into the continuous matrix in the spherical or worm-like nanodomains depending on the content of the triblock copolymer in the epoxy thermosets. It is found that a part of poly( $\epsilon$ -caprolactone) blocks were demixed from the epoxy matrix with the occurrence of curing reaction. The fractions of demixed PCL blocks were estimated according to the  $T_g$ -composition relation of the model binary blends of epoxy and PCL.

#### Acknowledgment

Financial support from Natural Science Foundation of China (No. 20474038 and 50873059) and National Basic Research Program of China (No. 2009CB930400) is gratefully acknowledged. The authors thank the Shanghai Synchrotron Radiation Facility under the projects of No. 0sr0260 & 10sr0126 and Shanghai Leading Academic Discipline Project (Project Number: B202) for partial support.

#### References

- Zheng S. In: Pascault JP, Williams RJJ, editors. Epoxy polymers: new materials and innovations. Weinheim: Wiley-VCH; 2010. p. 79–108.
- Ruiz-Pérez L, Royston GJ, Fairclough JA, Ryan AJ. Polymer 2008;49:4475.
- Hillmyer MA, Lipic PM, Hajduk DA, Almdal K, Bates FS. J Am Chem Soc 1997;119:2749.
- Lipic PM, Bates FS, Hillmyer MA. J Am Chem Soc 1998;120:8963.
- Mijovic J, Shen M, Sy JW, Mondragon I. Macromolecules 2000;33:5235.
- Grubbs RB, Dean JM, Broz ME, Bates FS. Macromolecules 2000;33:9522.
- Dean JM, Lipic PM, Grubbs RB, Cook RF, Bates FF. J Polym Sci Part B Polym Phys 2001;39:2996.
- Guo Q, Thomann R, Gronski W. Macromolecules 2002;35:3133.
- Ritzenthaler S, Court F, Girard-Reydet E, Leibler L, Pascault JP. Macromolecules 2002;35:6245.
- Ritzenthaler S, Court F, Girard-Reydet E, Leibler L, Pascault JP. Macromolecules 2003;36:118.
- Rebizant V, Abetz V, Tournihac T, Court F, Leibler L. Macromolecules 2003;36:9889.
- Dean JM, Verghese NE, Pham HQ, Bates FS. Macromolecules 2003;36:9267.
- Rebizant V, Venet AS, Tournihac F, Girard-Reydet E, Navarro C, Pascault JP, et al. Macromolecules 2004;37:8017.
- Dean JM, Grubbs RB, Saad W, Cook RF, Bates FS. J Polym Sci Part B Polym Phys 2003;41:2444.
- Wu J, Thio YS, Bates FS. J Polym Sci Part B Polym Phys 2005;43:1950.
- Zucchi IA, Galante MJ, Williams RJJ. Polymer 2005;46:2603.
- Thio YS, Wu J, Bates FS. Macromolecules 2006;39:7187.
- Serrano E, Tercjak A, Kortaberria G, Pomposo JA, Mecerreyes D, Zafeiropoulos NE, et al. Macromolecules 2006;39:2254.
- Ocando C, Serrano E, Tercjak A, Pena C, Kortaberria G, Calberg C, et al. Macromolecules 2007;40:4086.
- Maiez-Tribut S, Pascault JP, Soulec ER, Borrajo J, Williams RJJ. Macromolecules 2007;40:1268.
- Yi F, Zheng S, Liu T. J Phys Chem B 2009;113:11831.
- Hu D, Xu Z, Zeng K, Zheng S. Macromolecules 2010;43:2960.
- Zeng K, Wang L, Zheng S, Qian X. Polymer 2009;50:685.
- Gong W, Zeng K, Wang L, Zheng S. Polymer 2008;49:3318.
- Guo Q, Liu J, Chen L, Wang K. Polymer 2008;49:1737.
- Meng F, Zheng S, Zhang W, Li H, Liang Q. Macromolecules 2006;39:711.
- Meng F, Zheng S, Li H, Liang Q, Liu T. Macromolecules 2006;39:5072.
- Meng F, Zheng S, Liu T. Polymer 2006;47:7590.
- Sinturel C, Vayer M, Erre R, Amenitsch H. Macromolecules 2007;40:2532.
- Xu Z, Zheng S. Macromolecules 2007;40:2548.
- Meng F, Xu Z, Zheng S. Macromolecules 2008;41:1411.
- Fan W, Zheng S. Polymer 2008;49:3157.
- Fan W, Wang L, Zheng S. Macromolecules 2009;42:327.
- Ocando C, Tercjak A, Martin MD, Ramos JA, Campo M, Mondragon I. Macromolecules 2009;42:6215.
- Amendt MA, Chen L, Hillmyer MA. Macromolecules 2010;43:3924.
- Yang X, Yi F, Xin Z, Zheng S. Polymer 2009;49:4089.
- Flory PJ. Principles of polymer chemistry. Ithaca, NY: Cornell University Press; 1953.
- Wu Z, Grubbs RH. Macromolecules 1994;27:6700.
- Boschetti-de-Fierro A, Mueller AJ, Abetz V. Macromolecules 2007;40:1290.
- Binder WH, Kurzhals S, Pulamagatta B, Decker U, Pawar GM, Wang D, et al. Macromolecules 2008;41:8405.
- Kobayashi S, Kataoka H, Ishizone T, Kato T, Ono T, Kobukata S, et al. Macromolecules 2008;41:5502.
- Sanja ZN, Kupehela L. Polym Eng Sci 1976;28:1149.
- Ochi M, Okasaki M, Shimbo M. J Polym Sci Part B Polym Phys 1982;20:89.
- Shibanov YD, Godovsky YK. Prog Colloid Polym Sci 1989;80:110.
- Coleman MM, Painter PC. Prog Polym Sci 1995;20:1.
- Coleman MM, Graf JF, Painter PC. "Specific interactions and the miscibility of polymer blends". Lancaster, PA: Technomic Publishing; 1991.
- Yin M, Zheng S. Macromol Chem Phys 2005;206:929.
- Ni Y, Zheng S. Polymer 2005;46:5828.
- Fox TG. Bull Am Phys Soc 1956;1:123.
- Gordon M, Taylor JS. J Appl Chem 1952;2:496.
- Couchman PR. Macromolecules 1978;11:1156.